


Article

Critical Assessment of the Photocatalytic Reduction of Cr(VI) over Au/TiO₂

Anh Binh Ngo^{1,2}, Hong Lien Nguyen² and Dirk Hollmann^{3,4,*} ¹ Leibniz-Institute for Catalysis, Albert-Einstein-Str. 29a, D-18059 Rostock, Germany; anhbinh1208@gmail.com² School of Chemical Engineering, Hanoi University of Science and Technology, Dai Co Viet Street no.1, 100000 Ha Noi, Vietnam; lien.nguyenhong@hust.edu.vn³ Institute for Chemistry, University of Rostock, Albert-Einstein-Str. 3a, D-18059 Rostock, Germany⁴ Department of Life, Light and Matter, Interdisciplinary Faculty, University of Rostock, Albert-Einstein-Str. 25, D-18059 Rostock, Germany

* Correspondence: dirk.hollmann@uni-rostock.de

Received: 3 November 2018; Accepted: 23 November 2018; Published: 3 December 2018



Abstract: The purification of drinking water is one of the most urgent challenges in developing countries, for which the efficient removal of traces of heavy metals, e.g., Cr(IV), represents a key technology. This can be achieved via photocatalysis. In this study, we compare the performance of Au/TiO₂ to bare TiO₂ P25 catalysts. Furthermore, the influence of the sacrificial reagent citric acid under UV-Vis and Vis excitation was investigated and a detailed investigation of the catalysts before and after reaction was performed. During the photocatalytic reduction of Cr(IV) under acidic conditions, both leaching of Au, as well as absorption of Cr, occur, resulting in new catalyst systems obtained in situ.

Keywords: photocatalysis; Au/TiO₂; Cr(VI) reduction; citric acid; adsorption

1. Introduction

Nowadays, access to clean and accessible drinking water is one of the key challenges for humankind. Therefore, it was included among the 17 United Nations Sustainability Development Goals in 2017. Especially in developing countries, the rapid growth of industries led to an increase in wastewater without proper management and purification. Most of the water contaminants are harmful to both the environment and human health. Besides toxic organic compounds, heavy metals in high concentrations are also present in wastewater. Among these, Cr(VI) is considered to be one of the most toxic. Chromium compounds have been applied in many industries such as painting, furnace linings, tanning and dyeing processes, photography, and steel [1]. Chromium has two major stable oxidation states: Cr(VI) and Cr(III). While a moderate intake of Cr(III) is considered to be necessary for health, Cr(VI) is known to be very harmful even in small concentrations. Exposure (inhalation, ingestion, skin and eye contact) may cause cancer [2]. Therefore, Cr(VI) needs to be treated thoroughly before being released into the environment.

Many methods for Cr(VI) treatment have been investigated such as absorption by carbon materials with large surface area, ion exchange, membrane filtration, and chemical and electrochemical methods [3]. However, these methods have disadvantages: Absorption, ion exchange, and membrane filtration cannot thoroughly handle Cr(VI), since new toxic materials are produced. Chemical methods have the advantage of being simple but they imply the consumption of chemicals in a strongly acidic environment. Afterwards, the pH value must be raised to basic conditions to precipitate Cr(OH)₃. Electrochemical methods just remove Cr(VI) at high concentrations, hence, the wastewater from electroplating still has a significant amount of Cr(VI). Thus, it is of high interest to purify contaminated water that has a very small concentration of Cr (<50 ppm).

Photocatalysis is one promising method to reduce Cr(VI) to Cr(III). The advantage of this process is the complementary degradation of organic compounds together with the detoxification of heavy metals. One of the most popular photocatalysts is TiO₂ because of its high photoactivity, stability, non-toxicity, and low cost. However, with a large band gap energy (3.0–3.2 eV) TiO₂ can only be excited in the ultraviolet light region, making it ineffective under sunlight. In the past, many researchers tried to narrow the band gap energy of TiO₂ by doping with anions (e.g., N, C) [4] or cations (e.g., Sb, Cr, Fe, V, Mo) [5]. However, these methods had limited success, due to the fast recombination of conduction band electrons and holes [6]. Recently, a new generation of photocatalyst has been investigated by depositing noble metals e.g., Au on TiO₂ surfaces. The excitation of the so-called surface plasmon resonance (SPR) effect of the Au nanoparticles (NPs) enables the injection of hot electrons to TiO₂ in visible light [7].

During the photocatalytic reduction process, Cr(VI) is converted to Cr(V)/Cr(IV)/Cr(III) by conduction band electrons, see Figure 1 [8]. The photogenerated holes are able to oxidize H₂O and also to re-oxidize Cr(III) to Cr(VI), Cr(V), and Cr(IV) [9]. This re-oxidation reduces the overall efficiency of the Cr(VI) reduction process. Therefore, the presence of a sacrificial agent (SR), which is easier to oxidize than H₂O, prevents the re-oxidation of Cr(III) as well as decreases the occurrence of the recombination of electron and holes which can increase the photocatalytic performance.

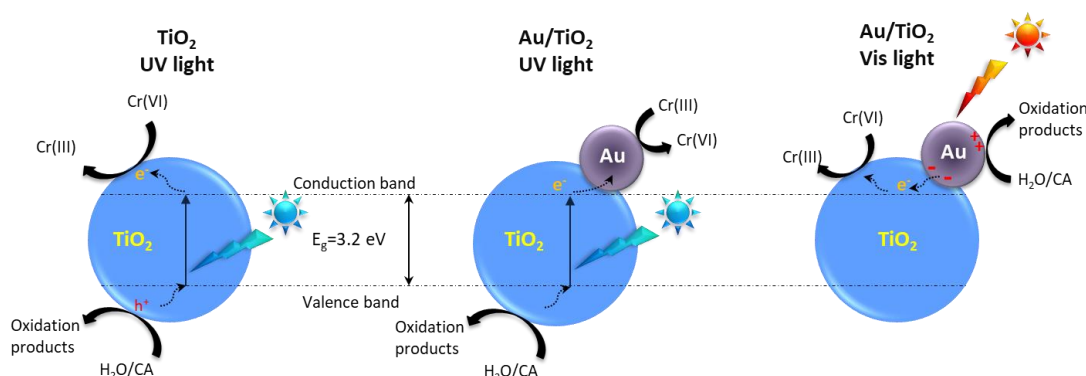


Figure 1. Photocatalytic mechanisms of Cr(VI) reduction by TiO₂ and Au/TiO₂ under UV-Vis and visible light irradiation.

Using citric acid (2-hydroxyl-propane-1,2,3-tricarboxylic acid) (CA), a common ingredient in cosmetics, pharmaceuticals, dietary supplements, and food industries, the photogenerated holes of TiO₂ can be easily oxidized [10]. Furthermore, citric acid can generate a stable Cr(V)-Cit complex which enables reaction monitoring by EPR spectroscopy [9].

We became interested in the Cr(VI) reduction during our investigation of proton reduction of water with advanced Au/TiO₂ [11]. Indeed, several publications have already described the improved catalytic Cr(VI) reduction on an Au/TiO₂ catalyst, see Figure 1 [12–15], but these are limited to special conditions, e.g., selected irradiation, pH, or SR. In principle, most electronic processes are known. However, investigation regarding the processes on the surface of the catalyst e.g., adsorption/desorption during irradiation is still needed. Unexpected results raised some questions about the role of Au, Cr, TiO₂(P25), and CA.

In this communication, we present a detailed investigation of the Cr(VI) reduction involving reactions with and without P25, Au/TiO₂ catalysts prepared by Deposition–Precipitation (DP) [11] (Au/P25-DP) as well as calcined Au/P25 DP (Au/P25-Cal) catalysts, see Figure 2. The Au/P25 catalyst, prepared by the DP method, comprises of gold hydroxide [11]. Calcination of this catalyst results in the formation of pure Au NPs on P25 (Au/P25-Cal).

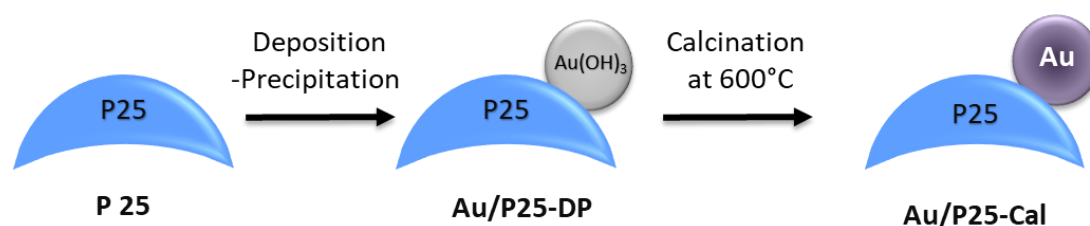


Figure 2. Preparation of the investigated catalyst.

All catalysts were examined with and without citric acid as the electron donor under UV-Vis and Vis irradiation. The catalysts were characterized before and after reaction by ICP and XRD. Additionally, selected catalysts were characterized by UV-Vis DRS, XPS, and TEM.

2. Results

2.1. Photocatalytic Activity

In general, the concentration of Cr(VI) was determined by UV-Vis without an additional complexation agent (absorbance at 350 nm, see more information in the experimental section). The catalytic performance was evaluated with a standard solution of Cr(VI) (20 ppm, pH 2, adjusted by H₂SO₄ 0.4 M). Three photocatalysts were investigated for Cr(VI) reduction: P25, Au/P25-DP, Au/P25-Cal. Photoreactions were carried out under UV-Vis (Xe-Lamp 300 W, no filter) or Vis excitation (cutoff filter 420 nm), in the absence of CA and the presence CA (molar ratio CA/Cr(VI) 25/1), see Table 1. After centrifugation, the conversion was detected after a 3-h reaction time by UV-Vis spectroscopy.

Table 1. Conversion of Cr(VI) with different conditions. ¹

Catalyst	No Light	No CA UV-Vis	No CA Vis	With CA UV-Vis	With CA Vis
P25	0	74	0	100 (70 ²)	92
Au/P25-DP	0	44	0	100	75
Au/P25-Cal	0	48	18	100	88
no catalysts	0	0	0	74	32

¹ Conversion after a 3-h reaction time in %; molar ratio CA:Cr(VI) 25:1. CA—Citric acid, Cal—calcined, DP—Deposition-Precipitation, see Figure 2. ² Conversion after recycling.

Under exclusion of light, no conversion was detected, indicating the negligible adsorption of Cr(VI) in the dark. Thus, the Cr(VI) conversion obtained occurs only by photoreaction. Under UV-Vis light (without CA) the photoactivity of P25 (75%) is much higher than with both Au/P25 catalysts (44% and 48%). This was a surprise since all other reports show a higher activity for Au/TiO₂ [12–15]. Under visible irradiation, only Au/P25-Cal showed photoactivity, indicating the necessity of the Au NPs on the catalyst. However, the efficiency of Cr(VI) reduction was moderate; after reaction for 3 h, just 18% of Cr(VI) was reduced. In contrast, the non-existent activity of Au/P25-DP in visible light indicates that under these conditions no Au NPs are formed from Au(OH)₃ under visible irradiation, which is in contrast to our recent investigations [11].

In the presence of citric acid (CA/Cr = 25/1), all catalysts completely reduced Cr(VI) to Cr(III) under UV light. It demonstrates the high necessity of citric acid as SA in photoreaction. Unexpectedly, citric acid alone can reduce Cr(VI) under UV-Vis. Here, 74% of Cr(VI) was reduced under UV-Vis light, and even 32% was reduced under visible light, raising the suspicion that a photoreaction between CA and Cr(VI) might take place. Indeed, with visible light and in the presence of CA, high conversions were still achieved even with pure P25 and Au/P25-DP. Although, Au/P25-DP and P25 have no absorption in the visible range. Even pure P25 showed a higher conversion than the Au-containing catalysts.

Thus, the roles of these catalysts could be clarified by the results from the catalytic characterization methods, as described below.

2.2. Catalytic Characterization

2.2.1. UV-Vis Diffuse Reflectance Spectroscopy (UV-Vis DRS)

First, we were interested in the change of the absorbance of the SPR band in the Au/TiO₂ catalysts by UV-Vis spectroscopy, see Figure 3. All photocatalysts showed strong absorbance in the region below 387 nm due to the P25 support. Au/TiO₂-DP (before reaction) shows a broad absorption band in the visible region due to Au(OH)₃. After reaction under UV light, a broad absorption at 553 nm was observed, indicating the formation of a low amount of Au NPs generated by UV light [16]. Au/P25-Cal showed a maximum absorbance at 600 nm, indicating the formation and agglomeration towards large Au NPs [11]. However, the absorbance in the visible region of Au/P25-Cal is much lower than in the UV region. This might be the reason for the low yield of Cr(VI) reduction under visible light (only 18%).

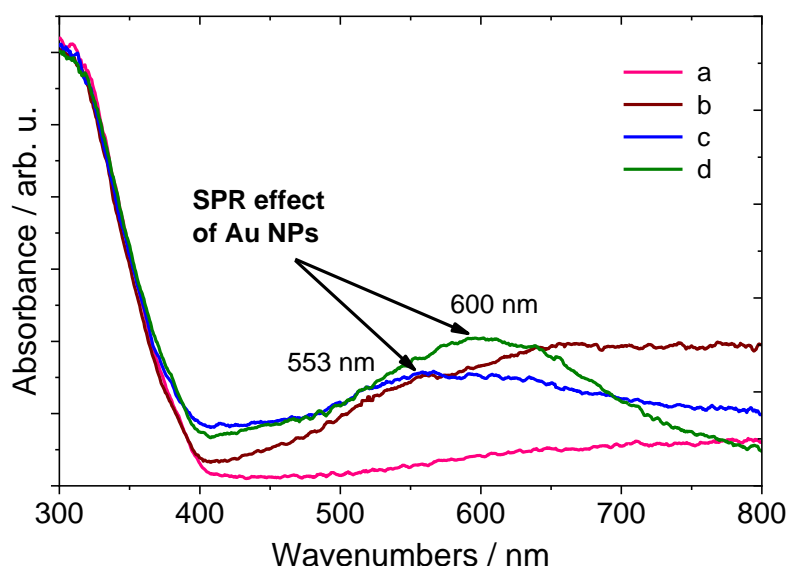


Figure 3. The UV-Vis diffuse reflectance measurement of photocatalysts; (a) P25, (b) Au/P25-DP, (c) Au/P25-DP after reaction under UV-Vis light, (d) Au/P25-Cal.

2.2.2. Chemical Composition of the Photocatalysts

Next, we analyzed the elemental composition of the catalysts before and after reaction by ICP-OES; the results of which are provided in Table 2. The main objective of this analysis was the detection of the Au that was still deposited on the surface after the reaction.

Table 2. Gold and chromium content on catalysts before and after reaction.

Catalyst	Before Reaction (wt%)	No CA UV-Vis (wt%)	No CA Vis (wt%)	With CA UV-Vis (wt%)	With CA Vis (wt%)
P25	Cr not determined (n.d.)	Cr 0.98	Cr n.d.	Cr 0.72	Cr 0.64
Au/P25-DP	Au 0.62	Au 0.16	Au 0.07	Au 0.18	Au 0.32
	Cr n.d.	Cr 0.23	Cr 0.11	Cr 0.70	Cr 0.45
Au/P25-Cal	Au 0.62	Au 0.51	Au 0.29	Au 0.35	Au 0.41
	Cr n.d.	Cr 0.61	Cr 0.31	Cr 0.25	Cr 0.61

By the used deposition—precipitation method, 0.62 wt% of Au can be deposited. However, a significant decrease of the gold content was observed after the reaction. Overall, the gold content

decreased more in Au/P25-DP than in the calcined sample. Without CA and visible light, nearly all gold was removed from the sample, which could explain the loss of activity. Indeed, in Au/P25-DP, Au(OH)₃ or Au₂O₃ is present on the surface. This Au can be easily dissolved in an acidic environment or chelated and leached out by CA. This was not reported previously. However, if the Au NPs are already present in the starting material (e.g., Au/P25-Cal), then leaching and complexation are reduced.

Interestingly, we detected a significant amount of Cr in the catalyst sample after the reaction, see Table 2. Indeed, the results showed that, depending on the condition, chromium was chemically absorbed on the surface of the catalyst. In general, the chromium content on P25 was more than on the Au/P25 catalysts. With P25 and without CA under UV-VIS, nearly 100% of the converted Cr is present on the catalyst.

The valence state of the adsorbed chromium and gold on catalysts were measured by X-ray photoelectron spectroscopy, see Figure 4. Analysis from Au/P25-DP after reaction (no CA/with UV-VIS), showed the presence of Cr(III) (Cr 2p, 587 and 577.3 eV) and Au(0) (Au 4f, 87 and 83 eV) on the catalyst surface [11]. No Au(III) or Au(I) was detected which could be caused by the removal under acidic condition and/or CA.

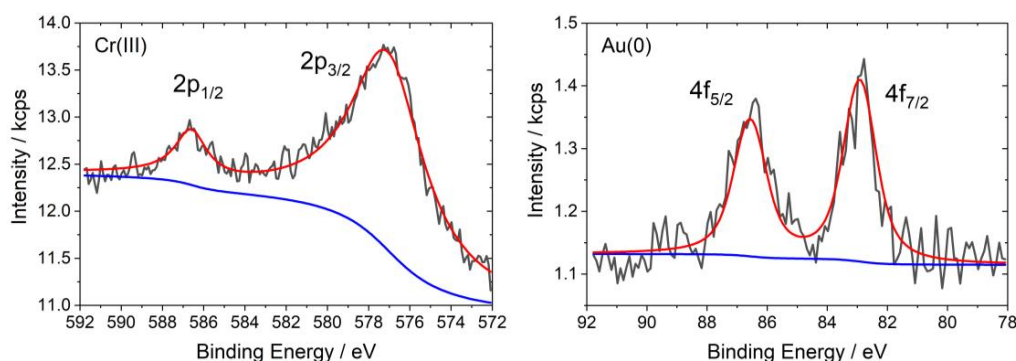


Figure 4. XPS results of Au/P25-DP after reaction under UV-Vis irradiation.

2.2.3. Crystal Structure and TEM

However, the state and distribution of Cr(III) is still unclear. Thus, the crystal structure of the photocatalysts were analyzed by powder X-ray diffraction. The results are shown in Figure 5.

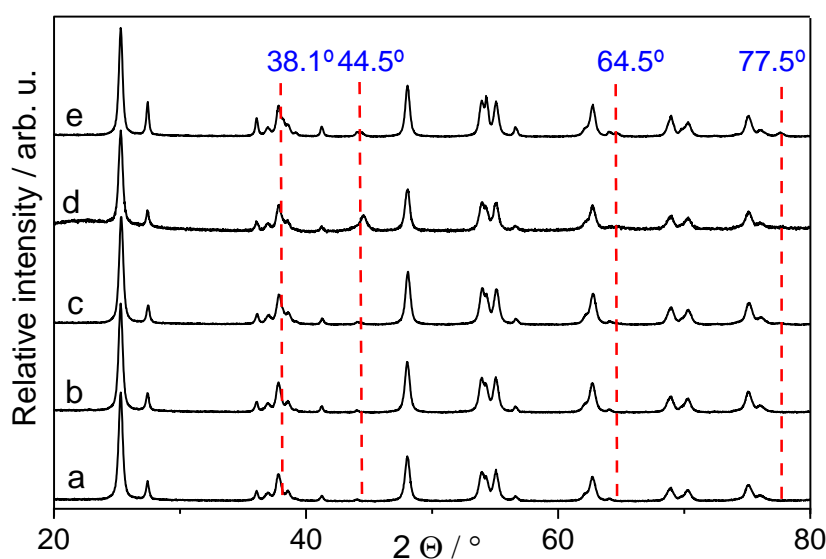


Figure 5. The Powder X-Ray diffraction pattern of photocatalysts, the diffraction pattern of the Au nanoparticle (NP) is marked; (a) P25, (b) P25 after reaction, (c) Au/P25-DP, (d) Au/P25-DP after reaction, (e) Au/P25-Cal.

The results of the X-ray diffraction analysis showed that the crystal structure of Anatase and Rutile in P25 did not change after modification by deposited Au NPs, nor after reaction with Cr(VI). Especially in Au/P25-Cal, see Figure 5e, and in Au/P25-DP after the reaction, see Figure 5d, Au NPs were detected due to the presence of characteristic diffraction peaks at 38.1° , 44.5° , 64.5° , and 77.5° . However, no reflections from Cr_2O_3 were detected. Although, the presence of Cr(III) on the catalyst after the reaction has been proved by ICP-OES and XPS. These apparently contradictory results could be explained by the dispersion of the low content of Cr(III) on the TiO_2 surface or the formation of amorphous Cr species.

To our disappointment, even transmission electron microscopy (TEM) cannot distinguish Cr and Ti from each other. The difference in the relative mass of Cr and Ti is too small to separate these elements. Furthermore, the amount of Cr is quite low. Only the distribution and size of the Au NPs (10–20 nm in Au/P25-DP under UV-Vis light) can be provided by TEM, see Figure 6, which is in accordance with the results published previously [11].

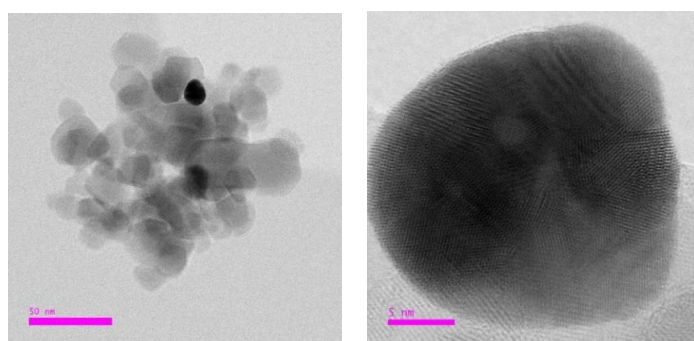


Figure 6. Transmission electron microscopy (TEM) for catalysts Au/P25-DP after reaction under UV-Vis irradiation.

2.2.4. Discussion of the Mechanism

The combined results indicate very important points which should always be addressed together with the Cr(IV) conversion, but have not been reported together before:

In the presence of CA or another SA, intermediate Cr(V)-CA complexes are formed which are photocatalytically (redox) active. This can distort the conversion of different photocatalysts, especially, under visible light.

The formation of the Cr(V)-CA complex was previously reported and can be proven by Electron Paramagnetic Resonance (EPR) Spectroscopy, see Figure 7A. The conversion of Cr(V)-CA under visible and UV-Vis light is shown in Figure 7B. Here, the Cr(V)-CA complex showed fast conversion in UV-Vis as well as slow conversion with visible light, even without P25. It can be assumed that the colored Cr(V)-CA complex can act as a photosensitizer.

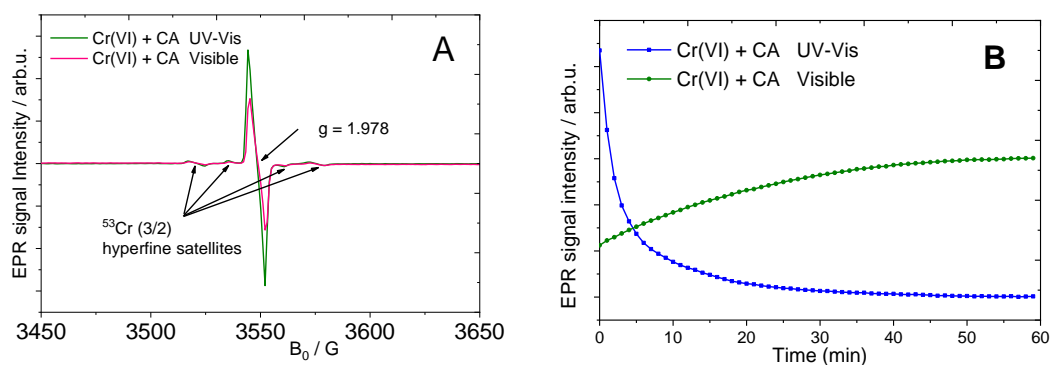


Figure 7. Cr(V)-CA complex detected by EPR spectroscopy (A), as well as Conversion of Cr(V)-CA (B) under UV-Vis and Vis irradiation.

In bare P25, the reduction of Cr(VI) occurs only at the active centers on the TiO₂ surface. This is associated with adsorption of the formed Cr(III) on the surface of TiO₂, see Figure 8. Depending on the condition, complete adsorption or partial dissolution can occur in the presence of CA.

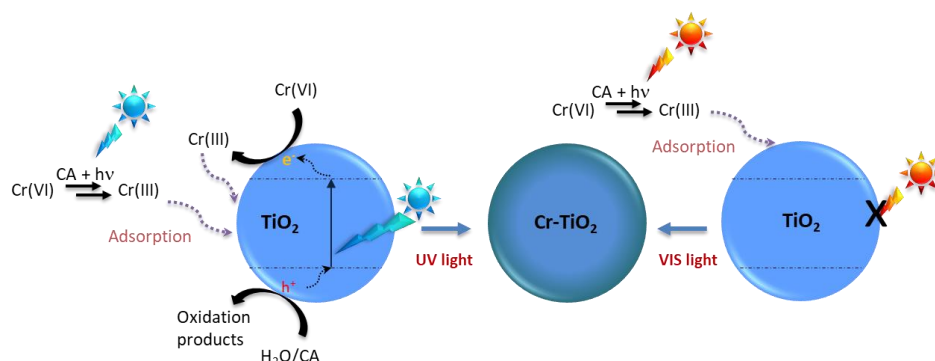


Figure 8. Proposed processes occurring on a bare P25 sample.

The newly formed Cr(III)/P25 catalyst has a lower activity than bare P25. For example, the reuse of P25 (after full conversion with CA and UV-VIS) results only in 70% conversion, see Table 1 and also the literature mentioned by Litter [8]. It can be assumed that the active reduction sites are blocked by Cr(III) adsorbates.

Under acidic conditions, no Au NPs are formed from Au(OH)₃. Instead, Au(OH)₃ is dissolved out from the TiO₂ surface, see Figure 9. This dissolution can be enhanced by the addition of CA. If Au NPs are present from the beginning, even partial dissolution of the Au NP can occur under acidic conditions. Under photocatalytic conditions, the reduction to Cr(III) occurs at the Au NP surface. Thus, the Au NP may be covered by Cr(III), see Figure 10. This is well known from the preparation of Cr/Rh core-shell catalysts [17–19]. However, the formation of an analog Au–Cr core-shell NPs still has to be proven.

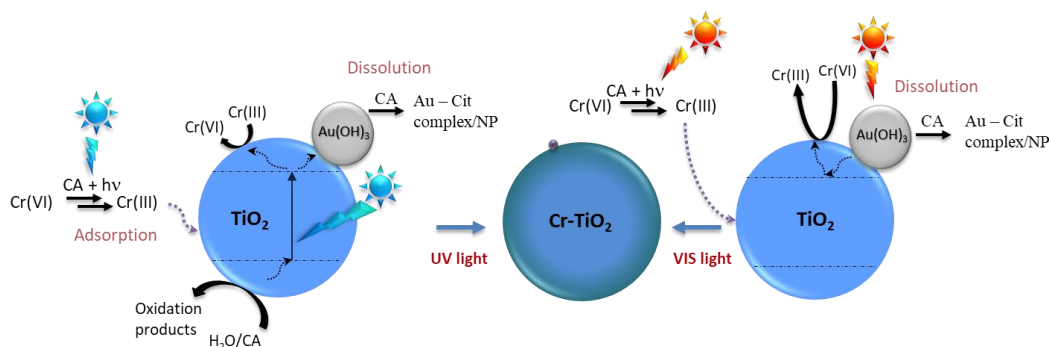


Figure 9. Proposed processes occurring on the Au/P25-DP sample.

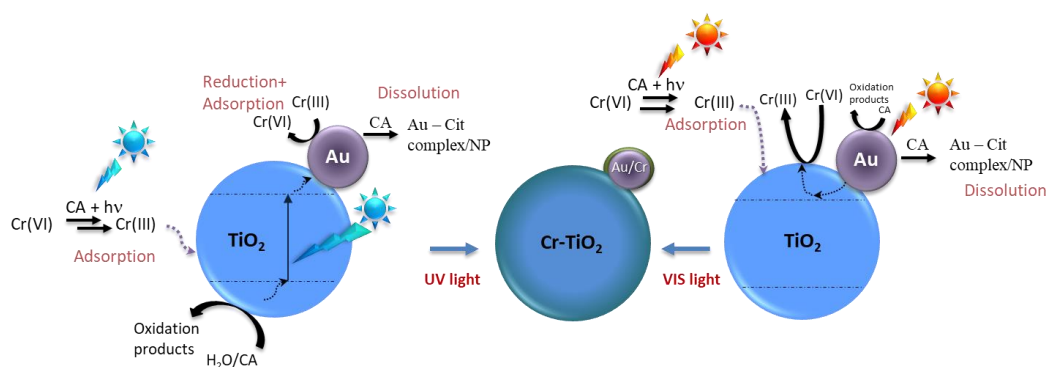


Figure 10. Proposed processes occurring on the Au/P25-DP sample.

In principle, the adsorption of Cr always results in a change of the photocatalysts independent from the substructure; therefore, a new Cr-containing photocatalyst is formed. Furthermore, assuming batch reactions, even this new catalyst will be continually changed during Cr(VI) reduction. This change of the catalyst systems should be considered quite critically and is not discussed in literature. In principle, under these conditions, TiO₂ and Au/TiO₂ catalysts are unsuitable for this type of photocatalytic reduction.

Very often, conversion of Cr(IV) is accompanied with an adsorption (mentioned as removal) [20]; although, these processes work in opposing directions. Thus, some strategies for the full recovery of the initial photocatalyst need to be developed in the future.

3. Materials and Methods

3.1. Materials

Au/TiO₂ catalysts were synthesized by TiO₂ P25 (anatase/rutile = 85:15, Evonik, S BET = 50 m²/g) and HAuCl₄·3H₂O (Aldrich, Germany). K₂Cr₂O₇ (CAS 7778-50-9) was used for Cr(VI) solution. Citric acid C₆H₈O₇ (CAS 5949-29-1) 99–102% was purchased from Alfa Aesar (Karlsruhe, Germany). H₂SO₄ and NaOH were used for adjusting the pH.

3.2. Catalytic Synthesis

Deposition of gold nanoparticles onto the TiO₂ surface was carried out by the deposition-precipitation method [11]. A total of 50 mL HAuCl₄ (5 mM) was heated to 70 °C then adjusted to pH 7 by 0.1 M NaOH. A total of 27 mL of Au-containing solution was added to 242 mL distilled water and stirred for 15 min at 70 °C prior to the addition 2.5 g of the P25 support. The resulting suspension was stirred for 1 h at 70 °C and for 1 h at 25 °C. The dry catalyst (Au/P25-DP) has Au(OH)₃ on the surface. Au NPs can generate on P25 by reaction under UV light or by calcination. At high temperature, Au(OH)₃ converts into Au₂O₃ and then to Au NP (Au/P25-Cal).

3.3. Catalytic Characterization

The elemental composition of catalysts was determined by ICP-OES using a Varian 715-ES ICP emission spectrometer (now Agilent, Germany) and ICP software. X-ray diffraction spectra were recorded using a VG Thermo ESCALAB 220iXL instrument (now Thermofisher Scientific, Germany) with monochromatic Al K α radiation (E = 1486.6 eV). Peaks were fitted by Gaussian-Lorentzian curves after Shirley background subtraction with a mean error in the binding energies of \pm (0.1–0.2) eV. Electron binding energy (XPS) was referenced to the adventitious carbon with a C 1s peak at 284.8 eV. For quantitative analysis, the peak areas were determined and divided by the element-specific Scofield factor and the analyzer-dependent transmission. Images of Au NPs and chromium on the TiO₂ surface were investigated by transmission electron microscopy (TEM) at 200 kV using a JEM-ARM200F instrument (JOEL, Peabody, MA, USA).

In situ EPR experiments were recorded by a Bruker EMX CW microspectrometer (Bruker, Germany) using an ER 4119HS-WI high-sensitivity optical resonator with a grid on the front side. The temperature was adjusted by a Bruker Digital Temperature Control System, ER4131VT. For light irradiation, the beam of a Lot-Oriel 300 W Xe lamp (LSB530) with a UV cutoff filter (GG42). The g values were calculated from the resonance field B₀ and the resonance frequency ν using the resonance condition.

3.4. Photocatalysis

Photoreactions were carried out in a vessel with a water jacket to keep the temperature of the solution at room temperature (25 °C) during the reaction. The light source was supplied by a Xe-arc lamp 300 W (LOT Oriel). The distance between the light source and the reactor was 11 cm, intensity was 411 mW/cm² in UV light and 365 mW/cm² in visible light. A 50 mg powder of

the catalyst was reacted with 40 mL Cr(VI), 20 ppm at pH 2 (adjusted by H₂SO₄ 4 M). The mixed suspensions were first magnetically stirred in the dark for 0.5 h to reach the adsorption–desorption equilibrium. The photoreaction was carried out in 3 h, with stirring during reaction time. After the reaction, the solution was filtered to measure the conversion. Cr₂O₇²⁻—a form of Cr(VI) in an acidic environment—has two maximum absorbances at 275 nm and 350 nm, see Figure 11A. Citric acid has a maximum absorbance at 275 nm. Compared to Cr(VI), Cr(III) (from Cr(NO₃)₃) has a maximum absorbance at 300 nm, 410 nm, and 577 nm. However, the absorbance intensity of Cr(III) can only be seen at high concentrations; >200 ppm, see Figure 11B. Low concentrations of Cr(III) (20 ppm or less) can almost not be detected. Therefore, the signal absorbance of the solution at 350 nm was used to measure the Cr(VI) conversion.

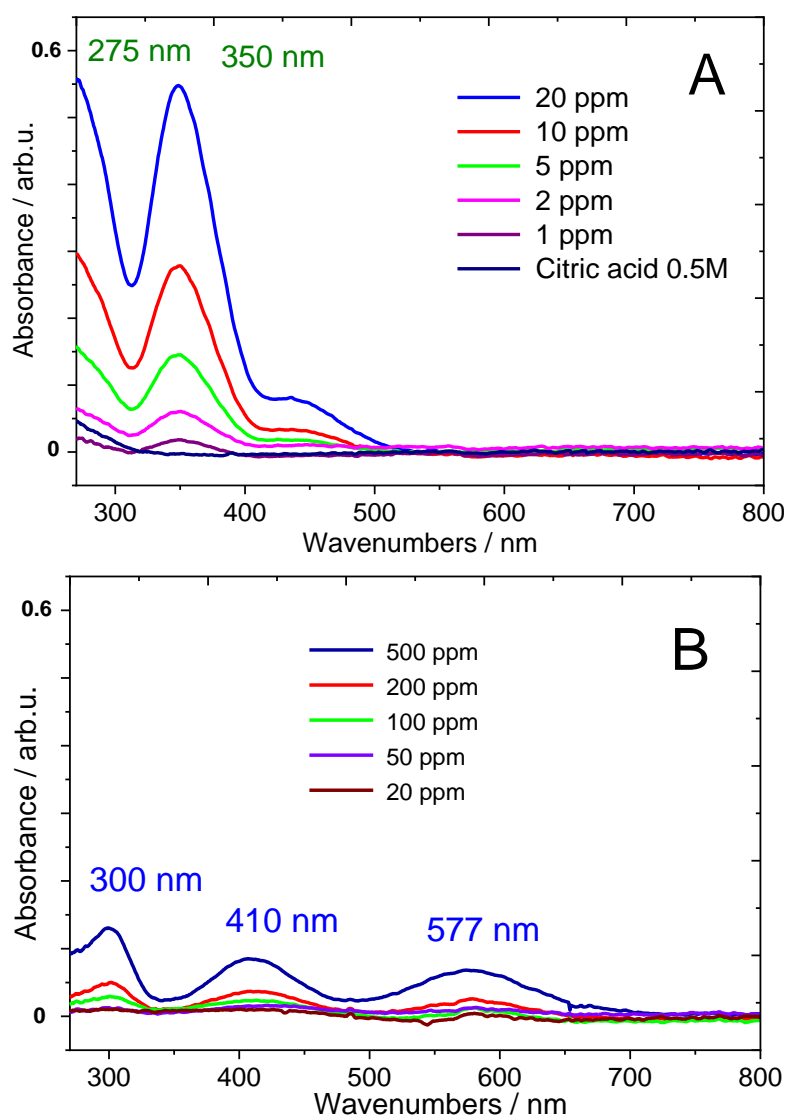


Figure 11. UV-Vis absorbance spectrum of Cr(VI) (A) and Cr(III) (B) at pH 2.

4. Conclusions

Within this study, the photocatalytic reduction ability towards Cr(VI) of Au/TiO₂ catalysts was compared to standard P25 catalysts. Depending on the method of synthesis, less reactivity (compare to P25) was obtained under UV-Vis excitation. The efficiency of Cr(VI) reduction increases strongly in the presence of citric acid under UV light. The Cr(VI) reduction by bare P25 is much better than Au/P25. Photocatalyst Au/P25-Cal (with Au NP) can reduce Cr(VI) under visible light, but only achieves low

conversion amounts. Interestingly, under irradiation even without a catalyst, a Cr(VI)-CA complex is formed which can act as a reductant itself.

These results can be explained by different parallel mechanisms occurring during catalysis. Partial dissolution of the gold hydroxide by citric acid (not reported before) as well as the reduction and desorption of Cr on the surface and/or Au nanoparticles need to be considered. Thus, under the reaction conditions (UV-Vis and Vis), complete new catalysts are formed containing Cr (and depleted of Au) on the surface. These mechanisms and processes resulting in the change of the catalyst system should be taken into account critically for recycling experiments as well as for the recovery of the original photocatalysts, but also for the use of other metallic co-catalysts such as Cu, Ag, and Pt.

Author Contributions: A.B.N. and D.H. designed the research; A.B.N. performed the research and analyzed the data; A.B.N. and D.H. wrote the paper; H.L.N. revised the paper. All authors read and approved the final manuscript.

Funding: This work has been supported by the RoHan Project funded by the German Academic Exchange Service (DAAD, No. 57315854) and the Federal Ministry for Economic Cooperation and Development (BMZ) inside the framework “SDG Bilateral Graduate School Program”.

Acknowledgments: D.H. thanks Carsten Robert Kreyenschulte for TEM measurements, Henrik Lund for XRD measurements, Anja Simmula for ICP-OES analysis, Angelika Brückner for the discussion during the project, and Esteban Mejia for correcting the manuscript.

Conflicts of Interest: The authors declare no conflict of interest.

References

1. Jacobs, J.A.; Testa, S.M. Overview of Chromium(VI) in the Environment: Background and History. In *Chromium(VI) Handbook*; Guertin, J., Jacobs, J.A., Avakian, C.P., Eds.; CRC Press: Boca Raton, FL, USA, 2004; Chapter 1.
2. Guertin, J. Toxicity and Health Effects of Chromium (All Oxidation States). In *Chromium(VI) Handbook*; Guertin, J., Jacobs, J.A., Avakian, C.P., Eds.; CRC Press: Boca Raton, FL, USA, 2004; Chapter 6.
3. Hawley, E.L.; Deeb, R.A.; Kavanaugh, M.C.; Jacobs, J.A. Treatment Technologies for Chromium(VI). In *Chromium(VI) Handbook*; Guertin, J., Jacobs, J.A., Avakian, C.P., Eds.; CRC Press: Boca Raton, FL, USA, 2004; Chapter 8.
4. Yuan, J.; Chen, M.; Shi, J.; Shangguan, W. Preparations and photocatalytic hydrogen evolution of N-doped TiO₂ from urea and titanium tetrachloride. *Int. J. Hydrog. Energy* **2006**, *31*, 1326–1331. [[CrossRef](#)]
5. Kato, H.; Kudo, A. Visible-Light-Response and Photocatalytic Activities of TiO₂ and SrTiO₃ Photocatalysts Codoped with Antimony and Chromium. *J. Phys. Chem. B* **2002**, *106*, 5029–5034. [[CrossRef](#)]
6. Daghri, R.; Drogui, P.; Robert, D. Modified TiO₂ For Environmental Photocatalytic Applications: A Review. *Ind. Eng. Chem. Res.* **2013**, *52*, 3581–3599. [[CrossRef](#)]
7. Tian, Y.; Tatsuma, T. Mechanisms and Applications of Plasmon-Induced Charge Separation at TiO₂ Films Loaded with Gold Nanoparticles. *J. Am. Chem. Soc.* **2005**, *127*, 7632–7637. [[CrossRef](#)] [[PubMed](#)]
8. Litter, M.I. Last advances on TiO₂-photocatalytic removal of chromium, uranium and arsenic. *Curr. Opin. Green Sustain. Chem.* **2017**, *6*, 150–158. [[CrossRef](#)]
9. Meichtry, J.M.; Brusa, M.; Mailhot, G.; Grela, M.A.; Litter, M.I. Heterogeneous photocatalysis of Cr(VI) in the presence of citric acid over TiO₂ particles: Relevance of Cr(V)–citrate complexes. *Appl. Catal. B* **2007**, *71*, 101–107. [[CrossRef](#)]
10. Meichtry, J.M.; Quici, N.; Mailhot, G.; Litter, M.I. Heterogeneous photocatalytic degradation of citric acid over TiO₂: II. Mechanism of citric acid degradation. *Appl. Catal. B* **2011**, *102*, 555–562. [[CrossRef](#)]
11. Priebe, J.B.; Radnik, J.; Lennox, A.J.J.; Pohl, M.-M.; Karnahl, M.; Hollmann, D.; Grabow, K.; Bentrup, U.; Junge, H.; Beller, M.; et al. Solar Hydrogen Production by Plasmonic Au–TiO₂ Catalysts: Impact of Synthesis Protocol and TiO₂ Phase on Charge Transfer Efficiency and H₂ Evolution Rates. *ACS Catal.* **2015**, 2137–2148. [[CrossRef](#)]
12. Dozzi, M.V.; Saccomanni, A.; Selli, E. Cr(VI) photocatalytic reduction: Effects of simultaneous organics oxidation and of gold nanoparticles photodeposition on TiO₂. *J. Hazard. Mater.* **2012**, *211–212*, 188–195. [[CrossRef](#)] [[PubMed](#)]

13. Liu, X.; Lv, T.; Liu, Y.; Pan, L.; Sun, Z. TiO₂-Au composite for efficient UV photocatalytic reduction of Cr(VI). *Desalin. Water Treat.* **2013**, *51*, 3889–3895. [[CrossRef](#)]
14. Tanaka, A.; Nakanishi, K.; Hamada, R.; Hashimoto, K.; Kominami, H. Simultaneous and Stoichiometric Water Oxidation and Cr(VI) Reduction in Aqueous Suspensions of Functionalized Plasmonic Photocatalyst Au/TiO₂-Pt under Irradiation of Green Light. *ACS Catal.* **2013**, *3*, 1886–1891. [[CrossRef](#)]
15. Luo, S.; Xiao, Y.; Yang, L.; Liu, C.; Su, F.; Li, Y.; Cai, Q.; Zeng, G. Simultaneous detoxification of hexavalent chromium and acid orange 7 by a novel Au/TiO₂ heterojunction composite nanotube arrays. *Sep. Purif. Technol.* **2011**, *79*, 85–91. [[CrossRef](#)]
16. Satoh, N.; Hasegawa, H.; Tsujii, K.; Kimura, K. Photoinduced Coagulation of Au Nanocolloids. *J. Phys. Chem.* **1994**, *98*, 2143–2147. [[CrossRef](#)]
17. Maeda, K.; Teramura, K.; Lu, D.; Saito, N.; Inoue, Y.; Domen, K. Roles of Rh/Cr₂O₃ (Core/Shell) Nanoparticles Photodeposited on Visible-Light-Responsive (Ga_{1-x}Zn_x)(N_{1-x}O_x) Solid Solutions in Photocatalytic Overall Water Splitting. *J. Phys. Chem. C* **2007**, *111*, 7554–7560. [[CrossRef](#)]
18. Soldat, J.; Marschall, R.; Wark, M. Improved overall water splitting with barium tantalate mixed oxide composites. *Chem. Sci.* **2014**, *5*, 3746–3752. [[CrossRef](#)]
19. Busser, G.W.; Mei, B.; Muhler, M. Optimizing the Deposition of Hydrogen Evolution Sites on Suspended Semiconductor Particles using On-Line Photocatalytic Reforming of Aqueous Methanol Solutions. *ChemSusChem* **2012**, *5*, 2200–2206. [[CrossRef](#)] [[PubMed](#)]
20. Yuan, X.; Feng, Z.; Zhao, J.; Niu, J.; Liu, J.; Peng, D.; Cheng, X. Significantly Enhanced Aqueous Cr(VI) Removal Performance of Bi/ZnO Nanocomposites via Synergistic Effect of Adsorption and SPR-Promoted Visible Light Photoreduction. *Catalysts* **2018**, *8*, 426. [[CrossRef](#)]



© 2018 by the authors. Licensee MDPI, Basel, Switzerland. This article is an open access article distributed under the terms and conditions of the Creative Commons Attribution (CC BY) license (<http://creativecommons.org/licenses/by/4.0/>).